

Stockholm, USITP 04
February 2004

BIRKHOFF'S POLYTOPE AND
UNISTOCHASTIC MATRICES
 $N = 3$ AND $N = 4$

Ingemar Bengtsson^{*1} Åsa Ericsson^{*2} Marek Kuś^{**3}

Wojciech Tadej^{***4} Karol Życzkowski^{****5}

**Stockholm University, AlbaNova, Fysikum, 106 91 Stockholm, Sweden.*

***Centrum Fizyki Teoretycznej, Polska Akademia Nauk, Al. Lotników
32/44, 02-668 Warszawa, Poland.*

****Cardinal Stefan Wyszyński University, Warszawa, Poland.*

*****Instytut Fizyki im. Smoluchowskiego, Uniwersytet Jagielloński, ul.
Reymonta 4, 30-059 Kraków, Poland.*

Abstract

The set of bistochastic or doubly stochastic $N \times N$ matrices form a convex set called Birkhoff's polytope, that we describe in some detail. Our problem is to characterize the set of unistochastic matrices as a subset of Birkhoff's polytope. For $N = 3$ we present fairly complete results. For $N = 4$ partial results are obtained. An interesting difference between the two cases is that there is a ball of unistochastic matrices around the van der Waerden matrix for $N = 3$, while this is not the case for $N = 4$.

¹ingemar@physto.se

²asae@physto.se

³marek@cft.edu.pl

⁴wtadej@wp.pl

⁵karol@tatry.if.uj.edu.pl

1. Introduction

There is a surprising variety of contexts in which unistochastic matrices arise, and any one of them may be taken as a motivation for the present study. But let us first define our terms: An $N \times N$ matrix B is said to be bistochastic if its matrix elements obey

$$\text{i: } B_{ij} \geq 0 \quad \text{ii: } \sum_i B_{ij} = 1 \quad \text{iii: } \sum_j B_{ij} = 1 . \quad (1)$$

The name ‘‘bistochastic’’ has to do with the fact that these matrices are usually supposed to act on probability distributions, thought of as N component vectors. The first condition ensures that positive vectors are transformed to positive vectors, the second that the sum of the components of the vectors remains invariant, and the third that the uniform distribution (a vector with all components equal) is a fixed point of the map. Hence a bistochastic matrix causes a kind of contraction of the probability simplex towards the uniform distribution. Condition iii is important because it guarantees that the map increases entropy. We obtain a bistochastic matrix if we start with a unitary matrix U and take the absolute value squared of its matrix elements,

$$B_{ij} = |U_{ij}|^2 . \quad (2)$$

For connoisseurs of linear algebra, B is the Hadamard product of U and its complex conjugate. If there exists such a U then B is said to be unistochastic. If U is also real, that is orthogonal, then B is said to be orthostochastic. Bistochastic matrices arise frequently in situations where probability distributions are changing, and we will soon see why one may want them to be unistochastic.

A somewhat distinguished bistochastic matrix is the van der Waerden matrix B_\star , whose matrix elements obey

$$B_{\star ij} = \frac{1}{N} . \quad (3)$$

The van der Waerden matrix is unistochastic. A corresponding unitary matrix is known as a complex Hadamard matrix. An example of a complex Hadamard matrix is the Fourier matrix, whose matrix elements are

$$U_{ij} = \frac{1}{\sqrt{N}} q^{ij} , \quad 0 \leq i, j \leq N - 1 . \quad (4)$$

Here $q = e^{2\pi i/N}$ is a root of unity. Complex Hadamard matrices have a long history in mathematics [1]. If the matrix U is also real it is referred to simply as a Hadamard matrix. By the way, the name of the van der Waerden matrix has to do with the conjecture that this matrix has the largest permanent of all bistochastic matrices; this is true but took a long time to prove [2].

It is clear that we now have two mathematical questions on our hands:

I: Given a bistochastic matrix, is it unistochastic?

II: If so, to what extent is U determined by B ?

The answer to question **I** turns out to depend on the bistochastic matrix chosen, so that in effect question **I** turns into the problem of characterizing the unistochastic subset of the set of all bistochastic matrices. But why are these questions interesting? The answer is that they naturally turn up in many contexts. Let us give a partial list of those.

The first context has to do with the foundations of quantum mechanics. Here there are a number of approaches where one begins by arguing that transition probabilities, suitably defined, form bistochastic matrices. In attempting to build some group structure into these transition probabilities one is then led to require that they form unistochastic matrices, and so one runs into question **I**. A sample of the literature includes Landé [3], Rovelli [4] and Khrennikov [5].

The second context is classical computer science, especially the theory of error correcting codes, design theory, and other areas of discrete mathematics where real Hadamard matrices are very useful. Hadamard conjectured that such matrices exist when $N = 2$ and $N = 4k$ [6]. The conjecture is still open, although much is known [7]. For explicit examples of real Hadamard matrices of all orders up to 256×256 , consult Sloane [8].

The third context is quantum information theory, where the restriction to real Hadamard matrices is somewhat unnatural. Complex Hadamard matrices have been studied in the quantum optics community in the guise of symmetric multiports; they are examples of specially designed unitary transformations that can be realized in the laboratory [9] [10]. There is also an interesting theorem [11] to the effect that the classification of all possible teleportation schemes can be reduced to the classification of all sets of maximally entangled bases; this is relevant here because such sets can be

obtained from the combination of a Latin square and a complex Hadamard matrix. The construction of all possible Latin squares has nothing to do with us here, but the construction of all complex Hadamard matrices certainly has. Mathematicians have studied this problem with various motivations [12] [13] [14] [15].

The fourth context is the attempt to formulate quantum mechanics on graphs (in the laboratory on thin strips of, say, gold film). Here question **I** arises as a question about what Markov processes that have a quantum counterpart in the given setting [16] [17] [18]. In this connection studies of the spectra and entropies of unistochastic matrices chosen at random have been made [19]; we will return to some of these issues below.

A fifth context is particle physics, where the interest centers on question **II**. Thus in the theory of weak interactions we encounter the unitary Kobayashi-Maskawa matrices (one for quarks and one for neutrinos), and Jarlskog raised the question to what extent such a matrix can be parametrized by the easily measured moduli of its matrix elements. The physically interesting case here is $N = 3$ [20], and possibly also $N = 4$ in case a fourth generation of quarks should be discovered [21]. (The same question occurs in scattering theory, with no restriction on N [22].)

We end the list of possible applications here, and turn to the organisation of our paper. In section 2 we describe the set of all bistochastic matrices \mathcal{B}_N . It is a convex polytope well known to practitioners of linear programming; it is sometimes called the assignment polytope because it arises in the problem of assigning N workers to N tasks, given their efficiency ratings for each task. We describe the cases $N = 3$ and $N = 4$ in detail ($N = 2$ is trivial). In section 3 we discuss some generalities concerning unistochastic matrices, and then we characterize the unistochastic subset for the case of $N = 3$. Most of our results can be found elsewhere but, we believe, not in this coherent form. In section 4 we address the same question for $N = 4$. This turns out to be a more difficult task, but at the end of this section there will be a proof that every neighbourhood of the van der Waerden matrix contains matrices that are not unistochastic. This is a striking difference to the $N = 3$ case. Section 5 summarises our conclusions. Some technical matters are found in three appendices. Our results on $N > 4$ will be reported in a separate publication [23].

2. Birkhoff's polytope

The set \mathcal{B}_N of bistochastic $N \times N$ matrices has $(N - 1)^2$ dimensions. To do this count, note that the last row and the last column are fixed by the conditions that the row and column sums should equal one. The remaining $(N - 1)^2$ entries can be chosen freely, within limits. Birkhoff proved that \mathcal{B}_N is a convex polytope whose extreme points, or corners, are the $N!$ permutation matrices [24]. All corners are equivalent in the sense that they can be taken into each other by means of orthogonal transformations. A bistochastic matrix belongs to the boundary of \mathcal{B}_N if and only if one of its entries is zero. The boundary consists of corners, edges, faces, 3-faces and so on; the highest dimensional faces are called facets and consist of matrices with only one zero entry. For a detailed account of \mathcal{B}_N , especially its face structure, see Brualdi et al. [25]. We will be even more detailed concerning \mathcal{B}_3 and \mathcal{B}_4 . For definiteness all 24 permutation matrices that occur when $N = 4$ are listed in Appendix A.

It is convenient to regard the convex polytope \mathcal{B}_N as a subset of a vector space with the van der Waerden matrix B_\star as its origin. The distance squared between two matrices is chosen to be

$$D^2(A, B) = \text{Tr}(A - B)(A^\dagger - B^\dagger) . \quad (5)$$

The distance squared between an arbitrary bistochastic matrix B and B_\star is then given by

$$D^2(B, B_\star) = \sum_{i,j} B_{ij}^2 - 1 . \quad (6)$$

In particular, the distance between B_\star and a corner of the polytope becomes $D = \sqrt{N - 1}$. Permutations of rows or columns are orthogonal transformations since they preserve distance and leave B_\star invariant. They also take permutation matrices (corners) into permutation matrices, hence they are symmetry operations of Birkhoff's polytope as well.

The (Shannon) entropy of a bistochastic matrix is defined as the entropy of the rows averaged over the columns,

$$S = -\frac{1}{N} \sum_i \sum_j B_{ij} \ln B_{ij} . \quad (7)$$

Its maximum value $\ln N$ is attained at B_\star . For some of its properties consult Słomczyński [26] et al. [19].

When $N = 2$ there are just two permutation matrices and \mathcal{B}_2 is a line segment between these two points. A general bistochastic matrix can be parametrized as

$$B = \begin{bmatrix} c^2 & s^2 \\ s^2 & c^2 \end{bmatrix}, \quad c \equiv \cos \theta, \quad s \equiv \sin \theta, \quad 0 \leq \theta \leq \frac{\pi}{2}. \quad (8)$$

When $N = 3$ we have six permutation matrices forming the vertices of a four dimensional polytope. It admits a simple description:

Theorem 1: The 6 corners of \mathcal{B}_3 are the corners of two equilateral triangles placed in two orthogonal 2-planes and centered at B_\star .

The proof is easy, using as corners the permutation matrices P_0, P_1, \dots, P_5 from Appendix A. The two equilateral triangles are the convex combinations

$$\Delta_1 = p_0 P_0 + p_3 P_3 + p_4 P_4 = \begin{bmatrix} p_0 & p_3 & p_4 \\ p_4 & p_0 & p_3 \\ p_3 & p_4 & p_0 \end{bmatrix}, \quad p_0 + p_3 + p_4 = 1 \quad (9)$$

and

$$\Delta_2 = p_1 P_1 + p_2 P_2 + p_5 P_5 = \begin{bmatrix} p_1 & p_2 & p_5 \\ p_2 & p_5 & p_1 \\ p_5 & p_1 & p_2 \end{bmatrix}, \quad p_1 + p_2 + p_5 = 1. \quad (10)$$

The calculation we have to do is to check that $D^2(P_0, P_3) = D^2(P_0, P_4) = D^2(P_3, P_4) = 6$ and similarly for the other triangle, and also that

$$\text{Tr}(\Delta_1 - B_\star)(\Delta_2^\dagger - B_\star^\dagger) = 0 \quad (11)$$

for all values of p_i . This is so.

There are thus 6 corners and $6 \cdot 5/2 = 15$ edges, all of which are extremal. The last is a rather exceptional property; in 3 dimensions only the simplex has it. There are 9 short edges of length squared $D^2 = 4$ and 6 long edges of length squared $D^2 = 6$, namely the sides of the two equilateral triangles.

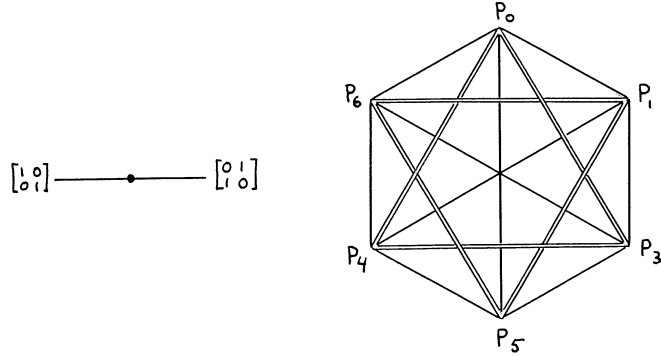


Figure 1: Left: Birkhoff's polytope for $N = 2$ (centered at B_*). Right: The graph of Birkhoff's polytope for $N = 3$; single lines have $D^2 = 4$ and double lines have $D^2 = 6$. The double edges form the triangles mentioned in Theorem 1.

A useful overview of \mathcal{B}_3 is given by its graph, where we exhibit all corners and all edges (see fig. 1). All the 2-faces are triangles with one long and two short edges. The 3-faces in a 4 dimensional polytope are called facets and are made of matrices with a single zero. They are irregular tetrahedra with two long edges, one from each equilateral triangle (see fig. 4).

The volume of \mathcal{B}_3 is readily computed because it can be triangulated using only three simplices. The total volume is $9/8$. As N grows the total volume of \mathcal{B}_N becomes increasingly hard to compute; mathematicians know it for $N \leq 10$ [27].

The next case is the 9 dimensional polytope \mathcal{B}_4 . It has 24 corners and 276 edges. The latter come in four types and we give the classification including the angle they subtend at \mathcal{B}_* and whether they consist of unistochastic matrices or not (see sections 3 and 4):

	Length squared	Unistochastic	Angle at origin	Number of edges
$4U$	4	Yes	Acute	72
6	6	No	90 degrees	96
8	8	No	Obtuse	72
$8U$	8	Yes	Obtuse	36

All edges except the $8U$ ones are extremal. The 2-faces consist of triangles and squares. (Interestingly, for all N it is true that the 2-faces of Birkhoff's

polytope \mathcal{B}_N are either triangles or rectangles [25].) There are 18 squares bounded by edges of type $4U$ and their diagonals are of type $8U$. Three squares meet at each corner. If we pick four permutation matrices we obtain a 3-face, with six exceptions. The exceptions form 6 regular tetrahedra centered at B_\star whose edges are non-extremal $8U$ edges. They are denoted T_i and explicitly listed in Appendix A; an example is

$$T_1 = p_0 P_0 + p_7 P_7 + p_{16} P_{16} + p_{23} P_{23} = \begin{bmatrix} p_0 & p_7 & p_{16} & p_{23} \\ p_7 & p_0 & p_{23} & p_{16} \\ p_{16} & p_{23} & p_0 & p_7 \\ p_{23} & p_{16} & p_7 & p_0 \end{bmatrix}. \quad (12)$$

When regular tetrahedra are mentioned below it is understood that we refer to one of these six. In a sense the structure can now be drawn; see fig. 2. The facets consist of matrices with one zero, so there are 16 facets.

A subset of \mathcal{B}_4 that has no counterpart for \mathcal{B}_3 is the set of matrices that are tensor products of two by two bistochastic matrices. This subset splits naturally into several two dimensional components, and it turns out that they sit in \mathcal{B}_4 as doubly ruled surfaces inside the regular tetrahedra. Thus the following matrix, parametrised with two angles, is a tensor product of two matrices of the form (8):

$$\begin{bmatrix} c_1^2 c_2^2 & c_1^2 s_2^2 & s_1^2 c_2^2 & s_1^2 s_2^2 \\ c_1^2 s_2^2 & c_1^2 c_2^2 & s_1^2 s_2^2 & s_1^2 c_2^2 \\ s_1^2 c_2^2 & s_1^2 s_2^2 & c_1^2 c_2^2 & c_1^2 s_2^2 \\ s_1^2 s_2^2 & s_1^2 c_2^2 & c_1^2 s_2^2 & c_1^2 c_2^2 \end{bmatrix}, \quad c_1 \equiv \cos \theta_1 \text{ etc.} \quad (13)$$

These matrices form a doubly ruled surface inside the regular tetrahedron (12), analogous to that depicted in fig. 4.

An interesting way to view \mathcal{B}_4 , and one that will recur in section 4, stems from the following observation:

Theorem 2: The 24 corners of \mathcal{B}_4 belong to a set of nine orthogonal hyperplanes through \mathcal{B}_\star . Each regular tetrahedron belongs to six hyperplanes and contains the normal vectors of the remaining three hyperplanes. Each hyperplane contains four regular tetrahedra and its normal vector is the intersection of the remaining two regular tetrahedra.

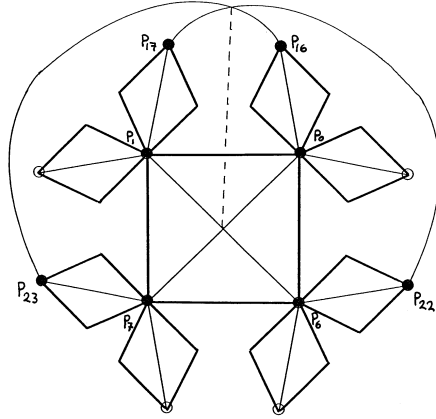


Figure 2: How to begin to draw the surface of \mathcal{B}_4 . Two tetrahedra whose edges are the non-extremal diagonals of squares are shown. The dashed line goes through the polytope; it connects the midpoints of two opposing $8U$ edges of two tetrahedra that are otherwise disjoint.

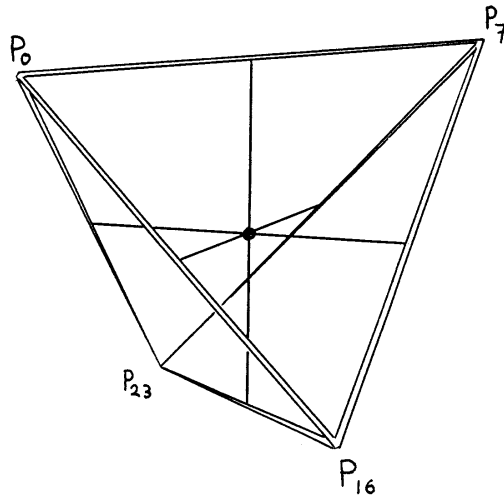


Figure 3: A regular tetrahedron centered at B_* . It contains the normal vectors of three orthogonal hyperplanes and belongs entirely to another six. There are six such regular tetrahedra and pairs of them intersect along the normal vectors they contain. (Note that the dashed line in Fig. 2 represents such a normal vector.)

Again the proof is a simple calculation, once the explicit form of the hyperplanes is known. They are denoted Π_i and listed in Appendix A. From now on, “hyperplane” always refers to one of these nine. Fig. 3 in a sense illustrates the theorem.

It is quite helpful to have an incidence table for tetrahedra and hyperplanes available. It is

	Π_1	Π_2	Π_3	Π_4	Π_5	Π_6	Π_7	Π_8	Π_9	
T_1		X	X	X		X	X	X		
T_2		X	X	X	X		X		X	
T_3	X		X		X	X	X	X		
T_4	X	X			X	X	X		X	
T_5	X		X	X	X			X	X	
T_6	X	X		X		X		X	X	

(14)

where the tetrahedra T_i and the hyperplanes Π_i are listed in Appendix A.

For later purposes we will need some information about exactly how the hyperplanes divide the space into 2^9 hyperoctants. For this reason we look at the rays

$$B_i(t) = B_\star + tV_i , \tag{15}$$

where V_i is a vector constructed in terms of the normal vectors n_1, \dots, n_9 of the hyperplanes (see Appendix B), namely

$$V_1 \equiv n_1 + n_2 + n_3 + n_4 + n_5 + n_6 + n_7 + n_8 + n_9 = \frac{1}{4} \begin{bmatrix} 9 & -3 & -3 & -3 \\ -3 & 1 & 1 & 1 \\ -3 & 1 & 1 & 1 \\ -3 & 1 & 1 & 1 \end{bmatrix} \tag{16}$$

$$V_2 \equiv n_1 + n_2 + n_3 + n_4 + n_5 + n_6 + n_7 + n_8 - n_9 = \frac{1}{4} \begin{bmatrix} 7 & -1 & -1 & -5 \\ -1 & -1 & -1 & 3 \\ -1 & -1 & -1 & 3 \\ -5 & 3 & 3 & -1 \end{bmatrix} \tag{17}$$

$$V_3 \equiv n_1 + n_2 + n_3 + n_4 - n_5 + n_6 + n_7 + n_8 - n_9 = \frac{1}{4} \begin{bmatrix} 5 & 1 & -3 & -3 \\ 1 & -3 & 1 & 1 \\ -3 & 1 & -3 & 5 \\ -3 & 1 & 5 & -3 \end{bmatrix}. \quad (18)$$

All other cases can be obtained from one of these three by permutations of rows and columns. The various hyperoctants are convex cones centered on these rays. This gives a classification of the hyperoctants into six different types (since the parameter t can be positive or negative) called respectively type I_{\pm} , II_{\pm} and III_{\pm} . Type I has 16 representatives and is especially noteworthy. For type I_- the centered ray hits the boundary in the center of one of the 16 facets, at the matrix $B_1(-\frac{1}{9})$. In the other direction we also hit quite distinguished points. There are 16 ways of setting one entry of a bistochastic matrix equal to one, and this gives rise to 16 copies of \mathcal{B}_3 sitting in the boundary of \mathcal{B}_4 . For the octants I_+ the centered ray hits the boundary precisely at the center of such a \mathcal{B}_3 , at the matrix $B_1(\frac{1}{3})$.

In section 4 we will see how the structure of the unistochastic subset is related to the structure of Birkhoff's polytope, and in particular to the features we have stressed.

3. The unistochastic subset, mostly $N = 3$

Let us begin with some generalities concerning the unistochastic subset \mathcal{U}_N of \mathcal{B}_N . The dimension of \mathcal{B}_N is $(N - 1)^2$ and the dimension of $U(N)$ is N^2 . Therefore the map $U(N) \rightarrow \mathcal{B}_N$ cannot be one-to-one. Now it is clear that multiplying a row or a column by a phase factor—an operation that we refer to as rephasing—will result in the same bistochastic matrix via eq. (2). Therefore the map is naturally defined as a map from a double coset space to \mathcal{B}_N . The double coset space is

$$U(1) \times \cdots \times U(1) \setminus U(N) / U(1) \times \cdots \times U(1) , \quad (19)$$

with N $U(1)$ factors on the right and $N - 1$ factors on the left, say. The dimension of this set is $(N - 1)^2$ so now the dimensions match. There is a complication because the double coset space is not a smooth manifold. The action from the left of the $U(1)$ factors on the right coset space (in itself a well behaved flag manifold) has fixed points. These fixed points are easy to locate however (and always map to the boundary of \mathcal{B}_N), so that for most practical purposes we can think of our map as a map between smooth manifolds.

In general we will see that the image of our map is a proper subset of \mathcal{B}_N , and the map is many-to-one. There is not much we can usefully say about the general case, except for two remarks: The unistochastic subset \mathcal{U}_N has the full dimension $(N - 1)^2$ while the unistochastic subset of the boundary of \mathcal{B}_N has dimension $(N - 1)^2 - 2$; why this is so will presently become clear.

For $N = 2$ every bistochastic matrix is orthostochastic. A unitary matrix that maps to the matrix in eq. (8) is

$$U = \begin{bmatrix} c & s \\ s & -c \end{bmatrix} , \quad c \equiv \cos \theta , \quad s \equiv \sin \theta , \quad 0 \leq \theta \leq \frac{\pi}{2} . \quad (20)$$

The matrix is given in dephased form. This means that the first row and the first column is real and positive. This fixes the $U(1)$ factors mentioned above (unless there is a zero entry in one of these places) and from now on we will present all unitary matrices in this form. For any N it is straightforward to check whether a given edge of \mathcal{B}_N is unistochastic. For $N = 3$ the edges of length squared equal to 4 are unistochastic, and for $N = 4$ we have the results given in table (12).

Given a 3×3 bistochastic matrix it is easy to check whether it is unistochastic or not [28] [20]. We form the moduli $r_{ij} = \sqrt{B_{ij}}$ and write down the matrix

$$U = \begin{bmatrix} r_{00} & r_{01} & \bullet \\ r_{10} & r_{11}e^{i\phi_{11}} & \bullet \\ r_{20} & r_{21}e^{i\phi_{21}} & \bullet \end{bmatrix} \quad (21)$$

If this matrix is unitary the original matrix is unistochastic. The unitarity conditions simply say that the first two columns are orthogonal; the last column by construction has the right moduli and does not impose any further restrictions. Therefore the problem is to form a triangle from three line segments of given lengths

$$L_0 = r_{00}r_{01} \quad L_1 = r_{10}r_{11} \quad L_2 = r_{20}r_{21} . \quad (22)$$

This is possible if and only if the ‘‘chain–links’’ conditions are fulfilled, i.e.

$$|L_1 - L_2| \leq L_0 \leq L_1 + L_2 . \quad (23)$$

The bistochastic matrix corresponding to U sits at the boundary of \mathcal{U}_3 if and only if one of these inequalities is saturated. When eq. (23) holds the solution is

$$\cos \phi_{11} = \frac{L_2^2 - L_0^2 - L_1^2}{2L_0L_1} \quad \cos \phi_{21} = \frac{L_1^2 - L_2^2 - L_0^2}{2L_0L_2} \quad (24)$$

$$\cos(\phi_{11} - \phi_{21}) = \frac{L_0^2 - L_1^2 - L_2^2}{2L_1L_2} . \quad (25)$$

There is a two-fold ambiguity (corresponding to taking the complex conjugate of the matrix, $U \rightarrow U^*$). The area A of the triangle is easily computed and the chain–links conditions are equivalent to the single inequality $A \geq 0$. As a matter of fact we can form six so called unitarity triangles in this way, depending on what pair of columns or rows that we choose. Although their shapes differ their area is the same, by unitarity [20].

Because we can easily decide if a given matrix is unistochastic, it is easy to characterize the unistochastic set \mathcal{U}_3 . We single out the following facts (some of which are known [28]) for attention:

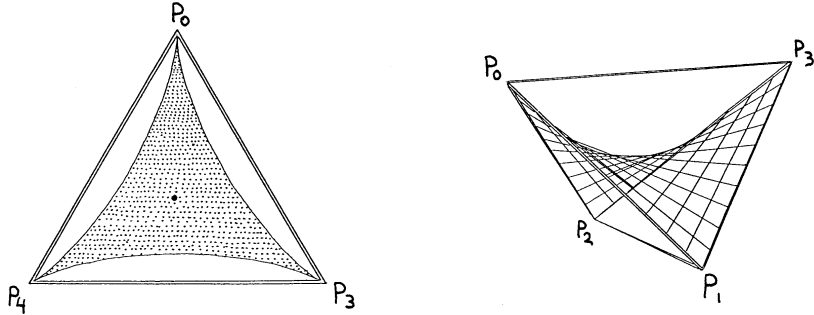


Figure 4: Birkhoff's polytope for $N = 3$. Left: One of the two orthogonal equilateral triangles centered at B_* , with its unistochastic subset (the boundary is the famous hypocycloid). Right: A facet, an irregular tetrahedron, with its doubly ruled surface of unistochastic matrices.

Theorem 3: The unistochastic subset \mathcal{U}_3 of \mathcal{B}_3 is a non-convex star shaped four dimensional set whose boundary consists of the set of orthostochastic matrices. It contains a unistochastic ball of maximal radius $\sqrt{2}/3$, centered at B_* . The set meets the boundary of \mathcal{B}_3 in a doubly ruled surface in each facet.

The relative volume of the unistochastic subset is, according to our numerics,

$$\frac{\text{vol}(\mathcal{U}_3)}{\text{vol}(\mathcal{B}_3)} \approx 0.7520 \pm 0.0005 . \quad (26)$$

We did not attempt an analytical calculation; details of our numerics are in Appendix B.

Theorem 3 is easy to prove. To see that \mathcal{U}_3 is non-convex we just draw its intersection with one of the equilateral triangles that went into the definition of the polytope, and look at it (see fig. 4). An amusing side remark is that the boundary of the unistochastic set in this picture is a 3-hypocycloid [19]. It can be obtained by rolling a circle of radius $1/3$ inside the unit circle. The maximal unistochastic ball is centered at B_* and touches the boundary at the hypocycloid, as one might guess from the picture; its radius was deduced from results presented in ref. [29]. To see that the boundary consists of orthostochastic matrices is the observation that when the chain-links conditions are saturated the phases in U will equal ± 1 . That the

set is star shaped then follows from an explicit check that there is only one orthostochastic matrix on any ray from B_* . Finally fig. 4 includes an explicit picture of the unistochastic subset of a facet. The reason why it has codimension one is that a matrix on the boundary of \mathcal{B}_N has a zero entry, which means that the number of phases available in the dephased unitary matrix drops with one, and then the dimension of the unistochastic set also drops with one; the argument goes through for any N .

Finally let us make some remarks on entropy. We compare the Shannon entropy averaged over \mathcal{B}_3 using the flat measure, the Shannon entropy averaged over \mathcal{U}_3 also using the flat measure, and the maximal Shannon entropy S_{\max} . Numerically we find that

$$\langle S \rangle_{\mathcal{B}_3} \approx 0.883 \quad \text{and} \quad \langle S \rangle_{\mathcal{U}_3} \approx 0.908 \quad (27)$$

with all digits significant. Observe that the latter average is larger since some matrices of small entropy close to the boundary of \mathcal{B}_3 are not unistochastic and do not contribute to the average over \mathcal{U}_3 . The above data may be compared with the maximal possible entropy $S_{\max} = \ln 3 \approx 1.099$, attained at B_* , and also with

$$\langle S \rangle_{\text{Haar}} = \frac{1}{2} + \frac{1}{3} \approx 0.833 \quad , \quad (28)$$

which is the average taken over \mathcal{U}_3 with respect to measure induced by the Haar measure on $U(3)$. This analytical result follows directly from the work of Jones, who computed the average entropy of squared components of complex random vectors [30]. It is easy to see that the two averages coincide. For details of our numerics consult Appendix B.

4. The unistochastic subset, mostly $N = 4$

The case $N = 4$ is more difficult. It is also clear from the outset that it will be qualitatively different—thus the dimension of the orthogonal group is too small for the boundary of the unistochastic set \mathcal{U}_4 to be formed by orthostochastic matrices alone. There are other differences too, as we will see.

Given a bistochastic matrix we can again define $r_{ij} = \sqrt{B_{ij}}$ and consider

$$U = \begin{bmatrix} r_{00} & r_{01} & r_{02} & \bullet \\ r_{10} & r_{11}e^{i\phi_{11}} & r_{12}e^{i\phi_{12}} & \bullet \\ r_{20} & r_{21}e^{i\phi_{21}} & r_{22}e^{i\phi_{22}} & \bullet \\ r_{30} & r_{31}e^{i\phi_{31}} & r_{32}e^{i\phi_{32}} & \bullet \end{bmatrix} \quad (29)$$

Phases must now be chosen so that this matrix is unitary, and more especially so that the three columns we focus on are orthogonal. Geometrically this is the problem of forming three quadrilaterals with their sides given and six free angles. This is not a simple problem, and in practice we have to resort to numerics to see whether a given bistochastic matrix is unistochastic (see Appendix B for details). There are some easy special cases though. One easy case is that of a matrix belonging to the boundary of \mathcal{B}_N . Then the matrix U must contain one zero entry and when we check the orthogonality of our three columns two of the equations reduce to the problem of forming triangles, so that the angles are completely fixed when we consider the final orthogonality relation. Another easy case concerns the regular tetrahedra. They turn out to consist of orthostochastic matrices; for the example given in eq. (12) a corresponding orthonormal matrix is

$$O_1 = \begin{bmatrix} \sqrt{p_0} & \sqrt{p_7} & \sqrt{p_{16}} & \sqrt{p_{23}} \\ \sqrt{p_7} & -\sqrt{p_0} & -\sqrt{p_{23}} & \sqrt{p_{16}} \\ \sqrt{p_{16}} & \sqrt{p_{23}} & -\sqrt{p_0} & -\sqrt{p_7} \\ \sqrt{p_{23}} & -\sqrt{p_{16}} & \sqrt{p_7} & -\sqrt{p_0} \end{bmatrix}. \quad (30)$$

This saturates a bound saying that the maximum number of $N \times N$ permutation matrices whose convex hull is unistochastic is not larger than $2^{\lfloor \frac{N}{2} \rfloor}$, where $\lfloor N/2 \rfloor$ denotes the integer part of $N/2$ [31].

Let us now turn our attention to B_\star . Hadamard [6] observed that up to permutations of rows and columns the most general form of the complex

Hadamard matrix is

$$H(\phi) = \frac{1}{2} \begin{bmatrix} 1 & 1 & 1 & 1 \\ 1 & e^{i\phi} & -1 & -e^{i\phi} \\ 1 & -1 & 1 & -1 \\ 1 & -e^{i\phi} & -1 & e^{i\phi} \end{bmatrix} \quad (31)$$

One can show that this is a geodesic in $U(N)$. The news, compared to $N = 3$, is that B_\star is orthostochastic because $H(0)$ is real. Moreover there is a continuous set of dephased unitaries mapping to the same B . In a calculational *tour de force*, Auberson et al. [21] were able to determine all bistochastic matrices whose dephased unitary preimages contain a continuous ambiguity (and they found that the ambiguity is given by one parameter in all cases). There are three such families. Using the notation of ref. [21] they consist of matrices of the following form:

$$\text{Type A: } \begin{bmatrix} a & b & c & d \\ b & a & d & c \\ e & f & g & h \\ f & e & h & g \end{bmatrix} \quad \text{Type C: } \begin{bmatrix} a & a & \frac{1}{2} - a & \frac{1}{2} - a \\ b & b & \frac{1}{2} - b & \frac{1}{2} - b \\ c & c & \frac{1}{2} - c & \frac{1}{2} - c \\ d & d & \frac{1}{2} - d & \frac{1}{2} - d \end{bmatrix} \quad (32)$$

$$\text{Type B: } \begin{bmatrix} s_1^2 s_2^2 & c_1^2 s_2^2 & c_3^2 c_2^2 & s_3^2 c_2^2 \\ s_1^2 c_2^2 & c_1^2 c_2^2 & c_3^2 s_2^2 & s_3^2 s_2^2 \\ c_1^2 c_4^2 & s_1^2 c_4^2 & s_3^2 s_4^2 & c_3^2 s_4^2 \\ c_1^2 s_4^2 & s_1^2 s_4^2 & s_3^2 c_4^2 & c_3^2 c_4^2 \end{bmatrix}. \quad (33)$$

Here $c_1 = \cos \theta_1$, $s_1 \equiv \sin \theta_1$, and so on. Type A consists of nine five dimensional sets, type B of nine four dimensional sets, and type C of six three dimensional sets. In trying to understand their location in \mathcal{B}_4 the observation in section 2 concerning the nine orthogonal hyperplanes begins to pay dividends. (In particular, consult the incidence table 14.) Type A consists of the linear subspaces obtained by taking all intersections of four hyperplanes that contain exactly two regular tetrahedra. Type C consists of the linear subspaces obtained by taking all intersections of six hyperplanes that contain no permutation matrices at all. Type B finally consists of curved manifolds confined to one hyperplane. Auberson's families are not exclusive. In particular tensor product matrices belong to families A and B, which means that there are two genuinely different ways of introducing a free phase in the

corresponding unitary matrix. Outside the three sets A , B and C Auberson et al. find a 12-fold discrete ambiguity in the dephased unitaries, dropping to 4-fold for symmetric matrices [21].

Tensor product matrices $B_4 = B_2 \otimes B'_2$ appear because $4 = 2 \times 2$ is a composite number. That they are always unistochastic follows from a more general result:

Lemma 1: Let B_K and B_M be unistochastic matrices of size K and M , respectively. Then the matrix $B_N = B_K \otimes B_M$ of size KM is unistochastic. The corresponding unitary matrices contain at least $(K - 1)(M - 1)$ free phases when dephased.

That B_N is unistochastic follows from properties of the Hadamard and the tensor products. By definition, the Hadamard product $A \circ B$ of two matrices is the matrix whose matrix elements are the products of the corresponding matrix elements of A and B . Then $B_K = U_K \circ U_K^*$ and $B_M = U_M \circ U_M^*$ implies that $B_N = (U_K \circ U_K^*) \otimes (U_M \circ U_M^*) = (U_K \otimes U_M) \circ (U_K^* \otimes U_M^*)$, so it is unistochastic. The existence of free phases is an easy generalization of proposition 2.9 in Haagerup [13].

The hyperplane structure of \mathcal{B}_4 reverberates in the structure of the unistochastic set in several ways. Let us consider how the tangent space of $U(N)$ behaves under the map to \mathcal{B}_N . In equations, this means that we fix a unitary matrix U_0 and expand

$$U(t) = e^{iht}U_0 = (1 + iht - \frac{1}{2}h^2t^2 + \dots)U_0 \quad (34)$$

where h is an Hermitian matrix. Then we study bistochastic matrices with elements $B_{ij}(t) = |U_{ij}(t)|^2$ to first order in t . The following general features are observed:

- Generically the tangent space of $U(N)$ maps onto the tangent space of \mathcal{B}_N . This implies that the dimension of the unistochastic set is equal to that of \mathcal{B}_N ; we checked this statement by generating unitary matrices at random using the Haar measure on the group.
- A matrix element in B receives a first order contribution only if it is non-vanishing. Hence the map of the tangent space of $U(N)$ to the

tangent space of \mathcal{B}_N is degenerate at the boundary of the polytope. In general such behaviour is to be expected at the boundary of the unistochastic set \mathcal{U}_N .

- If U_0 is real the map is degenerate in the sense that the tangent space maps to an $N(N - 1)/2$ dimensional subspace of the tangent space of \mathcal{B}_N .
- If U_0 maps to a corner of the polytope then the first order contributions vanish. To second order we pick up the tip of a convex cone whose extreme rays are the $N(N - 1)/2$ $4U$ edges emanating from that corner.

For $N = 4$ the story becomes interesting when we choose U_0 equal to the Hadamard matrix $H(\phi)$. Then we find that the tangent space at U_0 maps into one of the nine hyperplanes; which particular one depends on how we permute rows and columns in eq. (31). The question therefore arises whether the orthostochastic van der Waerden matrix belongs to the boundary of the unistochastic set—or not since *a priori* such degeneracies can occur also in the interior of the set.

We know that we can form curves of unistochastic matrices starting from B_\star and moving out into the nine hyperplanes. Can we form such curves that go directly out into one of the 2^9 hyperoctants? Here the division of the 2^9 hyperoctants into six different types becomes relevant. We have investigated whether their central rays given in eqs. (15-18) consist of unistochastic matrices, or not. Let us begin with the 16 hyperoctants of type I, where the central ray $B_1(t) = B_\star + tV_1$ hits the boundary in the center of one of the 16 \mathcal{B}_3 sitting in the boundary (at $t = 1/3$), and in the center of one of the 16 facets (at $t = -1/9$). Of these two points, the first is unistochastic, the second is not. A one parameter family of candidate unitary matrices that maps to the central ray is

$$U(t) = \frac{1}{2} \begin{bmatrix} \sqrt{1-3t} & \sqrt{1-3t} & \sqrt{1-3t} & \bullet \\ \sqrt{1+t} & \sqrt{1+te^{\phi_{11}}} & \sqrt{1+te^{i\phi_{12}}} & \bullet \\ \sqrt{1+t} & \sqrt{1+te^{i\phi_{21}}} & \sqrt{1+te^{\phi_{22}}} & \bullet \\ \sqrt{1+t} & \sqrt{1+te^{\phi_{31}}} & \sqrt{1+te^{i\phi_{32}}} & \bullet \end{bmatrix}, \quad (35)$$

where $t > 0$ and we permuted the columns relative to eq. (16) in order to get the unitarity equations in a pleasant form. (We do not need to give the

phases for the last column.) The conditions that the first three columns be orthogonal read

$$e^{i\phi_{11}} + e^{i\phi_{21}} + e^{i\phi_{31}} + L = 0 \quad (36)$$

$$e^{i\phi_{12}} + e^{i\phi_{22}} + e^{i\phi_{32}} + L = 0 \quad (37)$$

$$e^{i(\phi_{11}-\phi_{12})} + e^{i(\phi_{21}-\phi_{22})} + e^{i(\phi_{31}-\phi_{32})} + L = 0 \quad (38)$$

where

$$L = \frac{1 - 3t}{1 + t} . \quad (39)$$

In Appendix C we prove that the system of equations (36-38)

1. has no real solutions for $L > 1$,
2. for $0 < L < 1$ has the solution

$$\begin{aligned} \phi_{11} = 0 & \quad \phi_{21} = \phi & \quad \phi_{31} = -\phi \\ \phi_{12} = \phi & \quad \phi_{22} = 0 & \quad \phi_{32} = -\phi \end{aligned} , \quad \cos \phi = \frac{t - 1}{t + 1} = -\frac{L + 1}{2} . \quad (40)$$

It follows that the central ray is unistochastic for the hyperoctants of type I_+ (and the unitary matrices on the central ray tend to the real Hadamard matrix at $t = 0$). In the other direction the central ray is not unistochastic for type I_- . Thus we have proved

Theorem 4: For $N = 4$ there are non-unistochastic matrices in every neighbourhood of the van der Waerden matrix B_\star . At B_\star the map $U(4) \rightarrow \mathcal{B}_4$ aligns the tangent space of $U(4)$ with one of the nine orthogonal hyperplanes.

The structure of the unistochastic set is dramatically different depending on whether $N = 3$ or $N = 4$. It is only in the former case that there is a ball of unistochastic matrices surrounding B_\star . On the other hand, the hyperoctants are not empty—some of them do contain unistochastic matrices all the way down to B_\star .

Concerning the other hyperoctants, for types II_- , III_+ , and III_- the central rays hit the boundary of the polytope in points that are not unistochastic, but numerically we find that a part of the ray close to B_\star is unistochastic. For type II_+ we hit the boundary in a unistochastic point and numerically we find the entire ray to be unistochastic. There is still much that we do

not know. We do not know if the hyperoctants of type I_- are entirely free of unistochastic matrices, nor do we know if \mathcal{U}_4 is star shaped, or what its relative volume may be. What is clear from the results that we do have is that the global structure of Birkhoff's polytope reverberates in the structure of the unistochastic subset in an interesting way—it is a little bit like a nine dimensional snowflake, because the nine hyperplanes in \mathcal{B}_4 can be found through an analysis of the behaviour of \mathcal{U}_4 in the neighbourhood of B_\star .

5. Conclusions

Our reasons for studying the unistochastic subset of Birkhoff's polytope have been summarized in the introduction. Because the problem is a difficult one we concentrated on the cases $N = 3$ and $N = 4$. Our descriptions of Birkhoff's polytope for these two cases are given in Theorems 1 and 2, respectively, and a characterization sufficient for our purposes of the unistochastic set for $N = 3$ was given in Theorem 3. For $N = 4$ the dimension of the unistochastic set is again equal to that of the polytope itself, but its structure differs dramatically from the $N = 3$ case. In particular Theorem 4 states that for $N = 4$ there are non-unistochastic matrices in every neighbourhood of the van der Waerden matrix. Hence there does not exist a unistochastic ball surrounding the van der Waerden matrix. We observed that the structure of the unistochastic set at the center of the polytope reflects the global structure of the latter in an interesting way.

It is natural to ask to what extent the difference between the two cases reflects the fact that 3 is prime while 4 is not. Although this is not the place to discuss the cases $N > 4$, since some of us intend to do so in a separate publication [23], let us mention that the dimension of the unistochastic set is equal to that of \mathcal{B}_N for all values of N . On the other hand it is only in the case of N being a prime number that we have been able to show that there is a unistochastic ball surrounding the van der Waerden matrix.

Acknowledgements:

We thank Göran Björck, Prot Pakoński, Wojciech Słomczyński, and Gregor Tanner for discussions, Petre Dița for email correspondence, and Uffe Haagerup for supplying us with a copy of Petrescu's thesis. Financial support from the Swedish Research Council VR, and from the Polish Ministry of Scientific Research under grant No PBZ-MIN-008/P03/2003, is gratefully acknowledged.

Appendix A: Notation

An explicit list of permutation matrices for $N = 4$ is

$$P_0 = \begin{bmatrix} 1 & 0 & 0 & 0 \\ 0 & 1 & 0 & 0 \\ 0 & 0 & 1 & 0 \\ 0 & 0 & 0 & 1 \end{bmatrix} \quad P_1 = \begin{bmatrix} 1 & 0 & 0 & 0 \\ 0 & 1 & 0 & 0 \\ 0 & 0 & 0 & 1 \\ 0 & 0 & 1 & 0 \end{bmatrix} \quad P_2 = \begin{bmatrix} 1 & 0 & 0 & 0 \\ 0 & 0 & 1 & 0 \\ 0 & 1 & 0 & 0 \\ 0 & 0 & 0 & 1 \end{bmatrix} \quad (41)$$

$$P_3 = \begin{bmatrix} 1 & 0 & 0 & 0 \\ 0 & 0 & 1 & 0 \\ 0 & 0 & 0 & 1 \\ 0 & 1 & 0 & 0 \end{bmatrix} \quad P_4 = \begin{bmatrix} 1 & 0 & 0 & 0 \\ 0 & 0 & 0 & 1 \\ 0 & 1 & 0 & 0 \\ 0 & 0 & 1 & 0 \end{bmatrix} \quad P_5 = \begin{bmatrix} 1 & 0 & 0 & 0 \\ 0 & 0 & 0 & 1 \\ 0 & 0 & 1 & 0 \\ 0 & 1 & 0 & 0 \end{bmatrix} \quad (42)$$

$$P_6 = \begin{bmatrix} 0 & 1 & 0 & 0 \\ 1 & 0 & 0 & 0 \\ 0 & 0 & 1 & 0 \\ 0 & 0 & 0 & 1 \end{bmatrix} \quad P_7 = \begin{bmatrix} 0 & 1 & 0 & 0 \\ 1 & 0 & 0 & 0 \\ 0 & 0 & 0 & 1 \\ 0 & 0 & 1 & 0 \end{bmatrix} \quad P_8 = \begin{bmatrix} 0 & 1 & 0 & 0 \\ 0 & 0 & 1 & 0 \\ 1 & 0 & 0 & 0 \\ 0 & 0 & 0 & 1 \end{bmatrix} \quad (43)$$

$$P_9 = \begin{bmatrix} 0 & 1 & 0 & 0 \\ 0 & 0 & 1 & 0 \\ 0 & 0 & 0 & 1 \\ 1 & 0 & 0 & 0 \end{bmatrix} \quad P_{10} = \begin{bmatrix} 0 & 1 & 0 & 0 \\ 0 & 0 & 0 & 1 \\ 1 & 0 & 0 & 0 \\ 0 & 0 & 1 & 0 \end{bmatrix} \quad P_{11} = \begin{bmatrix} 0 & 1 & 0 & 0 \\ 0 & 0 & 0 & 1 \\ 0 & 0 & 1 & 0 \\ 1 & 0 & 0 & 0 \end{bmatrix} \quad (44)$$

$$P_{12} = \begin{bmatrix} 0 & 0 & 1 & 0 \\ 1 & 0 & 0 & 0 \\ 0 & 1 & 0 & 0 \\ 0 & 0 & 0 & 1 \end{bmatrix} \quad P_{13} = \begin{bmatrix} 0 & 0 & 1 & 0 \\ 1 & 0 & 0 & 0 \\ 0 & 0 & 0 & 1 \\ 0 & 1 & 0 & 0 \end{bmatrix} \quad P_{14} = \begin{bmatrix} 0 & 0 & 1 & 0 \\ 0 & 1 & 0 & 0 \\ 1 & 0 & 0 & 0 \\ 0 & 0 & 0 & 1 \end{bmatrix} \quad (45)$$

$$P_{15} = \begin{bmatrix} 0 & 0 & 1 & 0 \\ 0 & 1 & 0 & 0 \\ 0 & 0 & 0 & 1 \\ 1 & 0 & 0 & 0 \end{bmatrix} \quad P_{16} = \begin{bmatrix} 0 & 0 & 1 & 0 \\ 0 & 0 & 0 & 1 \\ 1 & 0 & 0 & 0 \\ 0 & 1 & 0 & 0 \end{bmatrix} \quad P_{17} = \begin{bmatrix} 0 & 0 & 1 & 0 \\ 0 & 0 & 0 & 1 \\ 0 & 1 & 0 & 0 \\ 1 & 0 & 0 & 0 \end{bmatrix} \quad (46)$$

$$P_{18} = \begin{bmatrix} 0 & 0 & 0 & 1 \\ 1 & 0 & 0 & 0 \\ 0 & 1 & 0 & 0 \\ 0 & 0 & 1 & 0 \end{bmatrix} \quad P_{19} = \begin{bmatrix} 0 & 0 & 0 & 1 \\ 1 & 0 & 0 & 0 \\ 0 & 0 & 1 & 0 \\ 0 & 1 & 0 & 0 \end{bmatrix} \quad P_{20} = \begin{bmatrix} 0 & 0 & 0 & 1 \\ 0 & 1 & 0 & 0 \\ 1 & 0 & 0 & 0 \\ 0 & 0 & 1 & 0 \end{bmatrix} \quad (47)$$

$$P_{21} = \begin{bmatrix} 0 & 0 & 0 & 1 \\ 0 & 1 & 0 & 0 \\ 0 & 0 & 1 & 0 \\ 1 & 0 & 0 & 0 \end{bmatrix} \quad P_{22} = \begin{bmatrix} 0 & 0 & 0 & 1 \\ 0 & 0 & 1 & 0 \\ 1 & 0 & 0 & 0 \\ 0 & 1 & 0 & 0 \end{bmatrix} \quad P_{23} = \begin{bmatrix} 0 & 0 & 0 & 1 \\ 0 & 0 & 1 & 0 \\ 0 & 1 & 0 & 0 \\ 1 & 0 & 0 & 0 \end{bmatrix} . \quad (48)$$

In Birkhoff's polytope these 24 matrices form the corners of 6 regular tetrahedra, namely the convex hulls of the sets

$$\begin{aligned} T_1 &= \{P_0, P_7, P_{16}, P_{23}\} & T_2 &= \{P_1, P_6, P_{17}, P_{22}\} \\ T_3 &= \{P_2, P_{10}, P_{13}, P_{21}\} & T_4 &= \{P_3, P_{11}, P_{12}, P_{20}\} \\ T_5 &= \{P_4, P_8, P_{15}, P_{19}\} & T_6 &= \{P_5, P_9, P_{14}, P_{18}\} . \end{aligned} \quad (49)$$

The nine hyperplanes mentioned in Theorem 2 consist of matrices of the form

$$\Pi_1 = \begin{bmatrix} B_{00} & B_{01} & \bullet & \bullet \\ B_{10} & B_{11} & \bullet & \bullet \\ \bullet & \bullet & \bullet & \bullet \\ \bullet & \bullet & \bullet & \bullet \end{bmatrix} \quad \Pi_2 = \begin{bmatrix} B_{00} & B_{01} & \bullet & \bullet \\ \bullet & \bullet & \bullet & \bullet \\ B_{20} & B_{21} & \bullet & \bullet \\ \bullet & \bullet & \bullet & \bullet \end{bmatrix} \quad (50)$$

$$\Pi_3 = \begin{bmatrix} B_{00} & B_{01} & \bullet & \bullet \\ \bullet & \bullet & \bullet & \bullet \\ \bullet & \bullet & \bullet & \bullet \\ B_{30} & B_{31} & \bullet & \bullet \end{bmatrix} \quad \Pi_4 = \begin{bmatrix} B_{00} & \bullet & B_{02} & \bullet \\ B_{10} & \bullet & B_{12} & \bullet \\ \bullet & \bullet & \bullet & \bullet \\ \bullet & \bullet & \bullet & \bullet \end{bmatrix} \quad (51)$$

$$\Pi_5 = \begin{bmatrix} B_{00} & \bullet & B_{02} & \bullet \\ \bullet & \bullet & \bullet & \bullet \\ B_{20} & \bullet & B_{22} & \bullet \\ \bullet & \bullet & \bullet & \bullet \end{bmatrix} \quad \Pi_6 = \begin{bmatrix} B_{00} & \bullet & B_{02} & \bullet \\ \bullet & \bullet & \bullet & \bullet \\ \bullet & \bullet & \bullet & \bullet \\ B_{30} & \bullet & B_{32} & \bullet \end{bmatrix} \quad (52)$$

$$\Pi_7 = \begin{bmatrix} B_{00} & \bullet & \bullet & B_{03} \\ B_{10} & \bullet & \bullet & B_{13} \\ \bullet & \bullet & \bullet & \bullet \\ \bullet & \bullet & \bullet & \bullet \end{bmatrix} \quad \Pi_8 = \begin{bmatrix} B_{00} & \bullet & \bullet & B_{03} \\ \bullet & \bullet & \bullet & \bullet \\ B_{20} & \bullet & \bullet & B_{23} \\ \bullet & \bullet & \bullet & \bullet \end{bmatrix} \quad (53)$$

$$\Pi_9 = \begin{bmatrix} B_{00} & \bullet & \bullet & B_{03} \\ \bullet & \bullet & \bullet & \bullet \\ \bullet & \bullet & \bullet & \bullet \\ B_{30} & \bullet & \bullet & B_{33} \end{bmatrix} \quad (54)$$

where the matrix elements that are explicitly written are assumed to sum to one (and similarly for the remaining three blocks taken separately).

The normal vectors of these hyperplanes are the matrices

$$n_1 = \frac{1}{4} \begin{bmatrix} 1 & 1 & -1 & -1 \\ 1 & 1 & -1 & -1 \\ -1 & -1 & 1 & 1 \\ -1 & -1 & 1 & 1 \end{bmatrix} \quad (55)$$

and so on.

Appendix B: Numerics

I. Average entropy in \mathcal{B}_3 .

To generate a random bistochastic matrix according to the flat measure on $\mathcal{B}_3 \subset \mathbb{R}^4$, we have drawn at random a point (x, y, z, t) in the 4-dimensional hypercube. It determines a minor of a $N = 3$ matrix, and the remaining five elements of B_3 may be determined by the unit sum conditions in eq. (1). Condition i is fulfilled if the sums in both rows and both columns of the minor does not exceed unity, and the sum of all four elements is not smaller than one. If this was the case, the random matrix B_3 was accepted to the ensemble of random bistochastic matrices. If additionally, the chain links condition (23) were satisfied, the matrix was accepted to the ensemble of unistochastic matrices, generated with respect to the flat measure on \mathcal{U}_3 . The mean entropies, (27), were computed by taking an average over both ensembles consisting of 10^7 random matrices, respectively.

II Numerical verification, whether a given bistochastic matrix B is unistochastic.

We have performed a random walk in the space of unitary matrices. Starting from an arbitrary random initial point U_0 we computed $B_0 = U_0 \circ U_0^*$ and its distance to the analyzed matrix, $D_0 = D(B_0, B)$, as defined in (5). We were fixing a small parameter $\alpha \approx 0.1$, generated a random Hermitian matrix H distributed according to the Gaussian unitary ensemble [32], and found a unitary perturbation $V = \exp(-\alpha H)$. The matrix $U_{n+1} = VU_n$ was accepted as a next point of the random trajectory, if the distance D_{n+1} was smaller than the previous one, D_n . If a certain number (say 100) of random matrices V did not allow us to decrease the distance, we were reducing the angle α by half, to start a finer search. A single run was stopped if the distance D was smaller than $\epsilon = 10^{-6}$ (numerical solution found), or α got smaller than a fixed cut off value (say $\alpha_{\min} = 10^{-4}$). In the latter case, the entire procedure was repeated a hundred times, starting from various unitary random matrices U_0 , generated according to the Haar measure on $U(4)$ [33]. The smallest distance D_{\min} and the closest unistochastic matrix $B_{\min} = U_n \circ \bar{U}_n$ was recorded.

To check the accuracy of the algorithm we constructed several random unistochastic matrices, $B = U \circ \bar{U}$, and verified that random walk procedure was giving their approximations with $D_{\min} < \epsilon$.

Appendix C: A system of equations

In order to curtail a plethora of indices in Eqs. (36-38) and ease the subsequent notation let us introduce shorthands: $\varphi_j = \phi_{j1}$, $\psi_j = -\phi_{j2}$, $j = 1, 2, 3$. With that the system rewrites as

$$e^{i\varphi_1} + e^{i\varphi_2} + e^{i\varphi_3} = -L \quad (56)$$

$$e^{i\psi_1} + e^{i\psi_2} + e^{i\psi_3} = -L \quad (57)$$

$$e^{i(\varphi_1+\psi_1)} + e^{i(\varphi_2+\psi_2)} + e^{i(\varphi_3+\psi_3)} = -L, \quad (58)$$

We shall prove the following:

Lemma: The system of equations (56-58)

1. has no real solutions for $L > 1$,
2. for $0 < L < 1$ has the solution

$$\begin{aligned} \varphi_1 = 0 \quad \varphi_2 = \phi \quad \varphi_3 = -\phi \\ \psi_1 = -\phi \quad \psi_2 = 0 \quad \psi_3 = \phi \end{aligned}, \quad \cos \phi = \frac{t-1}{t+1} = -\frac{L+1}{2}, \quad (59)$$

unique up to obvious permutations,

3. for $L = 0, 1$ has continuous families of solutions.

Indeed, each of the unimodal numbers $e^{i\varphi_k}$, $k = 1, 2, 3$ is a root of:

$$\begin{aligned} P(\lambda) &= (\lambda - e^{i\varphi_1})(\lambda - e^{i\varphi_2})(\lambda - e^{i\varphi_3}) & (60) \\ &= \lambda^3 - (e^{i\varphi_1} + e^{i\varphi_2} + e^{i\varphi_3})\lambda^2 + (e^{i(\varphi_1+\varphi_2)} + e^{i(\varphi_1+\varphi_3)} + e^{i(\varphi_2+\varphi_3)})\lambda - e^{i(\varphi_1+\varphi_2+\varphi_3)} \\ &= \lambda^3 - (e^{i\varphi_1} + e^{i\varphi_2} + e^{i\varphi_3})\lambda^2 + (e^{-i\varphi_3} + e^{-i\varphi_2} + e^{-i\varphi_1})e^{i(\varphi_1+\varphi_2+\varphi_3)}\lambda - e^{i(\varphi_1+\varphi_2+\varphi_3)} \\ &= \lambda^3 + \lambda^2 L - \lambda L e^{i\Phi} - e^{i\Phi} = \lambda^2(\lambda + L) - (1 + \lambda L)e^{i\Phi}, \end{aligned}$$

where $\Phi = \varphi_1 + \varphi_2 + \varphi_3$, and we used (56) and the reality of L . Thus each $\lambda = e^{i\varphi_k}$, ($k = 1, 2, 3$), fulfils:

$$\lambda^2(\lambda + L) = (1 + \lambda L)e^{i\Phi}. \quad (61)$$

Analogously, $\mu = e^{i\psi_k}$, ($k = 1, 2, 3$), fulfils

$$\mu^2(\mu + L) = (1 + \mu L)e^{i\Psi}, \quad (62)$$

with $\Psi = \psi_1 + \psi_2 + \psi_3$.

Observe now, that if $\lambda = e^{i\varphi_k}$ and $\mu = e^{i\psi_k}$ are solutions of (56-58) with the same number k , ($k = 1, 2, 3$) then, upon the same reasoning applied to (58), $\lambda\mu$ fulfils

$$\lambda^2\mu^2(\lambda\mu + L) = (1 + \lambda\mu L)e^{i(\Phi+\Psi)}. \quad (63)$$

Multiplying (61) by (62) and finally by (63) after exchanging its sides, we obtain, after division by $\lambda^2\mu^2e^{i(\Phi+\Psi)} \neq 0$,

$$(L + \lambda)(L + \mu)(L\lambda\mu + 1) = (L\lambda + 1)(L\mu + 1)(L + \lambda\mu), \quad (64)$$

which, upon substitution $\lambda = e^{i\varphi_k}$, $\mu = e^{i\psi_k}$ and putting everything on one side factorizes to

$$L(L - 1)(e^{i\varphi_k} - 1)(e^{i\psi_k} - 1)(e^{i(\varphi_k+\psi_k)} - 1) = 0, \quad (65)$$

(any computer symbolic manipulation program can be helpful in revealing (65) from (64)).

Hence, if $L \neq 0, 1$, then for each pair (φ_k, ψ_k) , $k = 1, 2, 3$, either: a) one of the angles is zero or b) they are opposite. The latter case can not occur for all three pairs since then $e^{i(\varphi_1+\psi_1)} + e^{i(\varphi_2+\psi_2)} + e^{i(\varphi_3+\psi_3)} = 3 \neq -L$, hence at least one of φ_k or ψ_k equals zero. Up to unimportant permutations we can assume $\varphi_3 = 0$, but then, since $e^{i\varphi_1} + e^{i\varphi_2} + e^{i\varphi_3} = -L \in \mathbb{R}$, we immediately get $\varphi_1 = -\varphi_2$. This determines also all other angles (also up to some unimportant permutation) and we end up with the solution announced in point 2. above as the only possibility, but such a solution exists only if $L \leq 1$.

To prove 3. observe that

1. for $L = 0$,

$$\varphi_1 = \varphi, \quad \varphi_2 = \varphi + 2\pi/3, \quad \varphi_3 = \varphi + 4\pi/3, \quad (66)$$

$$\psi_1 = \psi, \quad \psi_2 = \psi + 2\pi/3, \quad \psi_3 = \psi + 4\pi/3, \quad (67)$$

is a legitimate solution of (56-58) for arbitrary φ and ψ ,

2. for $L = 1$

$$\varphi_1 = \varphi, \quad \varphi_2 = \pi, \quad \varphi_3 = \varphi + \pi \quad (68)$$

$$\psi_1 = -\varphi + \pi, \quad \psi_2 = \pi, \quad \psi_3 = -\varphi, \quad (69)$$

is a solution for an arbitrary φ .

References

- [1] J. J. Sylvester, *Phil. Mag.* 34 (1867) 461.
- [2] J. H. van Lint, *Math. Intelligencer* 4 (1982) 72.
- [3] A. Landé, *From Dualism to Unity in Quantum Physics*, Cambridge U. P. (1960).
- [4] C. Rovelli, *Int. J. of Theor. Phys.* 35 (1996) 1637.
- [5] A. Khrennikov, *J. Phys.* A34 (2001) 1.

- [6] M. J. Hadamard, *Bull. Sci. Math.* 17 (1893) 240.
- [7] A. Hedayat and W. D. Wallis, *Ann. Stat.* 6 (1978) 1184.
- [8] N. J. A. Sloane's homepage, www.research.att.com/~njas/hadamard/index.html.
- [9] A. Zeilinger, M. Zukowski, M. A. Horne, H. J. Bernstein and D. M. Greenberger, in J. Anandan and J. L. Safko (eds): *Fundamental Aspects of Quantum Theory*, World Scientific, Singapore (1994).
- [10] P. Törmä, S. Stenholm and I. Jex, *Phys. Rev.* A52 (1995) 4853.
- [11] R. F. Werner, *J. Phys.* A34 (2001) 7081.
- [12] G. Björck and B. Saffari, *C. R. Acad. Sci. Paris, Sér. I* 320 (1995) 319.
- [13] U. Haagerup, in *Operator Algebras and Quantum Field Theory, Rome (1996)*, Internat. Press, Cambridge, MA (1997).
- [14] M. Petrescu, *Existence of continuous families of complex Hadamard matrices of certain prime dimensions and related results*, UCLA thesis, Los Angeles (1997).
- [15] P. Diță, arXiv: quant-ph/0212036.
- [16] G. Tanner, *J. Phys.* A34 (2001) 8485.
- [17] P. Pakoński, G. Tanner and K. Życzkowski, *J. Phys.* A34 (2001) 9303.
- [18] P. Pakoński, G. Tanner and K. Życzkowski, *J. Stat. Phys.* 111 (2003) 1331.
- [19] K. Życzkowski, M. Kuś, W. Słomczynski and H.-J. Sommers, *J. Phys.* A36 (2003) 3425.
- [20] C. Jarlskog and R. Stora, *Phys. Lett.* B208 (1988) 268.
- [21] G. Auberson, A. Martin and G. Mennessier, *Commun. Math. Phys.* 140 (1991) 523.
- [22] G. Mennessier and J. Nyuts, *J. Math. Phys.* 15 (1974) 1525.

- [23] W. Tadej et al., to appear.
- [24] G. Birkhoff, Univ. Nac. Tucumán Rev. A5 (1946) 147.
- [25] R. A. Brualdi and P. M. Gibson, J. Comb. Theory A22 (1977) 194.
- [26] W. Słomczyński, Open Sys. Inf. Dyn. 9 (2002) 201.
- [27] M. Beck and D. Pixton, arXiv: math.CO/0305322.
- [28] Y.-H. Au-Yeung and Y.-T. Poon, Lin. Alg. Appl. 27 (1979) 69.
- [29] H. G. Gadiyar, K. M. S. Maini, R. Padma and H. S. Sharatchandra, J. Phys. A36 (2003) L109.
- [30] K. R. W. Jones, J. Phys. A32 (1990) L1247.
- [31] Y.-H. Au-Yeung and C.-M. Cheng, Lin. Alg. Appl. 150 (1991) 243.
- [32] M. L. Mehta, *Random Matrices*, II ed., New York: Academic (1991).
- [33] M. Poźniak, K. Życzkowski, and M. Kuś, J. Phys. A31 (1998) 1059.